

# Bulge Elimination in Implicit Surface Blends

*Jules Bloomenthal*  
George Mason University  
Fairfax, Virginia USA  
jbloom@vit.gmu.edu

## Abstract

The relationship between surface bulges and several implicit blend techniques, particularly those based on convolution of a skeleton, is discussed. An examination of branching skeletons reveals that for two and three-dimensional skeletons, the surface will be bulge-free if elements are sufficiently large with respect to the convolution kernel.

**Keywords and Phrases:** implicit surface, blend, bulge, geometric modeling, skeleton, convolution.

## Introduction

Implicit surface blends can be obtained by combining *distance surfaces*. These are surfaces defined by distance to ‘skeletal’ elements such as points, line segments, polygons, or any free-form curve, surface, or volume. To illustrate, we consider distance to the planar curve shown below. Computing this distance is demanding [Bloomenthal 1989], [Schneider 1990], and often a piecewise linear approximation is substituted for the curve.

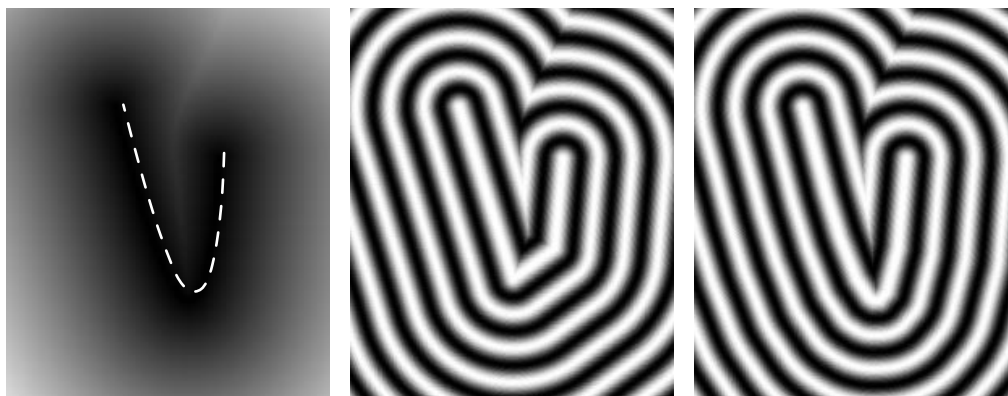


**Figure 1. Distance to a Curve**

*left: curve shown as dashed and distance shown as greyscale intensity*  
*middle and right: curve approximated by three and nine segments (contours emphasized)*

When distance to a curve is defined for three-dimensional points, the resulting implicit surface is a generalized cylinder. For a skeleton consisting of  $n$  segments, the implicit definition for a generalized cylinder with radius  $r$  is given by:

$$(1) \quad f(\mathbf{p}) = \min_i^n (d(\mathbf{p}, \text{segment}_i)^2)/r^2 - 1 = 0.$$

This computation requires a single comparison for each skeletal element and a single record in memory to store the smallest distance. The price for such simplicity is that the resulting surface encloses the simple union of the component primitive volumes. That is, if  $\mathbf{p}$  is within any individual primitive  $volume_i$  (defined by  $segment_i$ ), then  $d(\mathbf{p}, segment_i)^2/r^2 < 1$ ,  $f(\mathbf{p}) < 0$ , and  $\mathbf{p}$  is interior to the solid model. Thus,  $min$  in equation (1) corresponds to the *union* of individual volumes.

In general, distance surfaces are rounded wherever the skeleton is convex. Where the skeleton is concave, as along the upper part of the above curve, the surface (or contour) is tangent discontinuous and exhibits a crease, which we regard as undesirable. To eliminate creases, the primitive volumes must form a *blend*, rather than a union.

The blending of primitives in the context of solid modeling has received considerable study, as seen in a variety of recent work and the survey in [Woodwark 1986]. From these sources we learn that blended surfaces (or *blends*) are used in mechanical design to reduce stress, improve air or water flow, simplify casting, and improve aesthetics. Implicit blends may be categorized as rolling-ball, volume-bounded, range-controlled, and global [*ibid.*]. The first three produce surfaces that ‘heel’ to parts of individual primitive surfaces when those parts are sufficiently distant from other primitives.

We briefly review some aspects of algebraic blends, illustrating with the range-controlled, super-elliptic blend introduced in [Rockwood and Owen 1985]. Two implicit primitives,  $P_1$  and  $P_2$ , are combined according to a two-dimensional blending function,  $B$ :

$$(2) \quad f(\mathbf{p}) = B(P_1, P_2) = 1 - \left[1 - \frac{P_1(\mathbf{p})}{r_1}\right]_+^t - \left[1 - \frac{P_2(\mathbf{p})}{r_2}\right]_+^t, \text{ where}$$

$P_1, P_2$  are algebraic distances to skeletal elements 1 and 2, usually  $C^1$  continuous.

$r_1$  and  $r_2$  are the ranges of influence for primitives  $P_1$  and  $P_2$ ,

$[x]_+$  is  $\max(0, x)$ , and  $t$  is the ‘thumbweight.’

The blend is called super-elliptic because the graph of  $B(x, y)$  is super-elliptical (elliptical for  $t = 2$ ). Consider an example from [Rockwood 1989] that blends the unit sphere with a cylinder (centered on the  $x$ -axis with  $x \in [0, 2]$  and radius .4):

$$\text{sphere: } P_1(\mathbf{p}) = (\mathbf{p}_x^2 + \mathbf{p}_y^2 + \mathbf{p}_z^2)^{1/2} - 1$$

$$\text{cylinder: } P_2(\mathbf{p}) = \begin{cases} (\mathbf{p}_x^2 + \mathbf{p}_y^2 + \mathbf{p}_z^2)^{1/2} - .4, & \mathbf{p}_x < 0 \\ (\mathbf{p}_y^2 + \mathbf{p}_z^2)^{1/2} - .4, & 0 < \mathbf{p}_x < 2 \\ ((\mathbf{p}_x - 2)^2 + \mathbf{p}_y^2 + \mathbf{p}_z^2)^{1/2} - .4, & \mathbf{p}_x > 2 \end{cases}$$

The blend  $f(\mathbf{p}) = B(P_1(\mathbf{p}), P_2(\mathbf{p}))$ , with  $t = 3$ , is displayed below, left, as a cross-section in the  $xy$ -plane. Although  $P_1$  and  $P_2$  are linear with respect to distance,  $B$  is not, which accounts for the unequal contour spacing. The rendered surface is shown below, right.

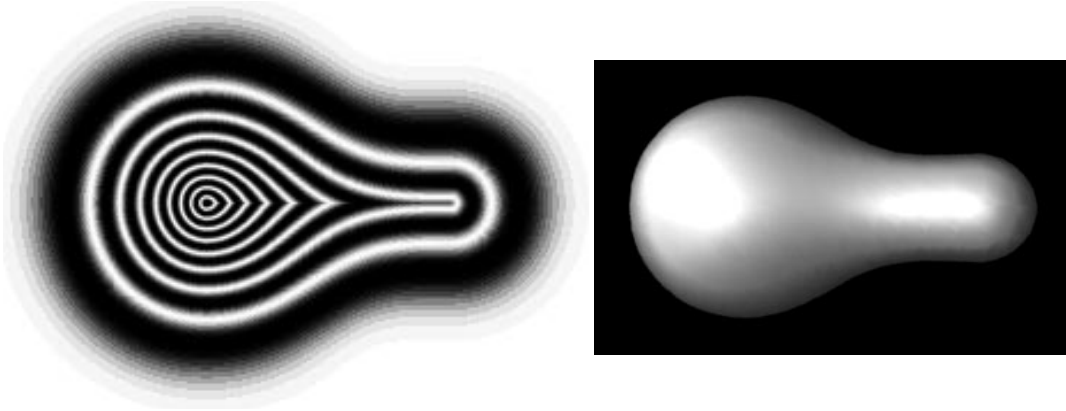


*Figure 2. Super-Elliptic Blend of Sphere and Cylinder*

Now consider two cylinders, one along the  $x$ -axis and one along the  $z$ -axis, as shown below, left. Contours of the blend, in the  $z = 0$  plane, are shown below, right, and exhibit a bulge where the cylinders intersect. Similar artifacts are visible in [Hoffmann and Hopcroft 1985] and [Middleditch and Sears 1985].

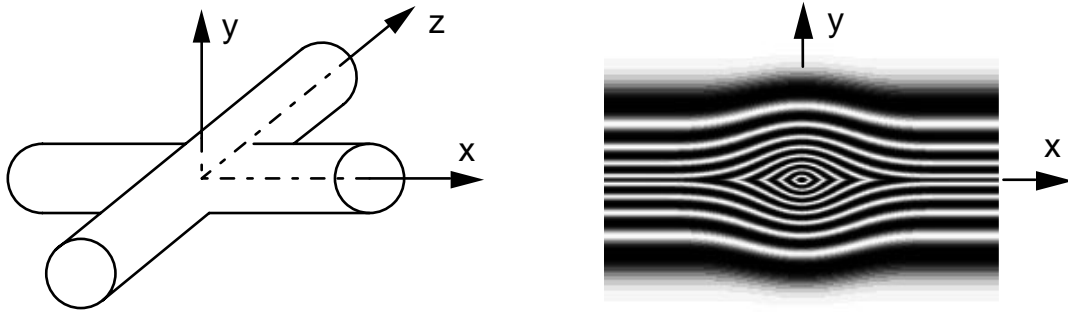


*Figure 3. Super-Elliptic Blend of Two Cylinders*

We have not encountered a formal definition of ‘bulge,’ and, so, we propose the following. A ‘surface bulge’ has a cross-section that exhibits negative, then positive, then negative curvature with respect to an underlying skeleton. For the super-elliptic blend, a bulge is to be expected, as those primitive values  $P_1$  and  $P_2$  that satisfy  $B(P_1, P_2) = 0$  do not sum to a constant. To compensate, a modification to the blend is discussed in [Rockwood 1989] whereby the range of a primitive is diminished according to the angle  $\theta$  between the gradients of the two primitives at a point  $\mathbf{p}$ :

$$(3) \quad B(P_1, P_2) = 1 - \left[ 1 - \frac{P_1(\mathbf{p})}{r_1(1 - \cos \theta)} \right]_+^t - \left[ 1 - \frac{P_2(\mathbf{p})}{r_2(1 - \cos \theta)} \right]_+^t$$

For  $\theta = 0$  the range is fully diminished and the simple union of the primitives results; for the concave condition  $\theta = 90^\circ$ , the range is undiminished, and a blend occurs. This

agrees with our previous observation that distance surfaces produce rounds along convex regions of a skeleton, but require blends along concave regions.  $\cos(\theta)$  must be non-negative, however, to avoid enlarging the primitive ranges. The following illustration depicts possible combinations of two primitives.

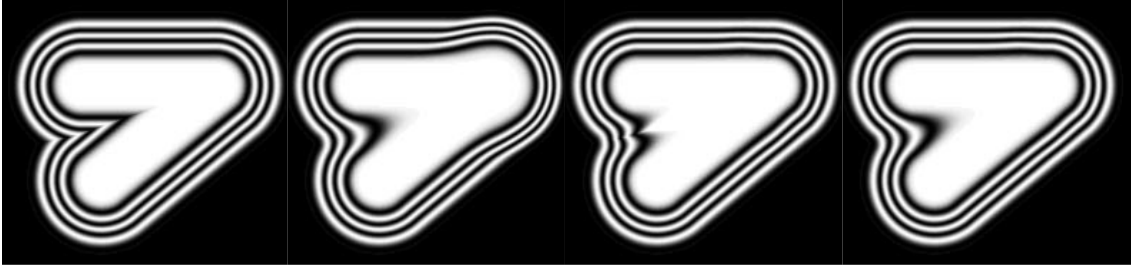


**Figure 4. Blend Based on Two Segments**

far left: simple union, left: bulging blend, right: use of  $\cos$ , far right: use of nonnegative  $\cos$

In [Rockwood 1989] the blend is extended to  $k$  primitives:

$$(4) \quad B_k = 1 - \sum_{i=1}^k \left[ 1 - \frac{P_i(\mathbf{p})}{r_i} \right]_+^t - c$$

The application of equation (3) to equation (4) is problematic, as  $\theta$  can be applied to two primitives only. Primitives could be functionally composed pairwise, but we prefer an independent evaluation of primitives, in arbitrary order. Such independence simplifies implementation and promotes extensibility, without influencing the design of an object.

## Convolution Surfaces

An independent evaluation of primitives is a feature of *convolution surfaces*, proposed as a bulge-free implicit blend technique in [Bloomenthal and Shoemake 1991]. Three-dimensional convolution treats a skeleton  $S$  as a set of points, each of which contributes to the implicit surface function according to its distance to  $\mathbf{p}$ . This is reminiscent of [Blinn 1982], in which an implicit surface is defined as the summation of terms, each based on the exponential (*i.e.*, *Gaussian*) decay of distance to a point:

$$(5) \quad f(\mathbf{p}) = c - \sum_i e^{-\|\mathbf{p} - \mathbf{s}_i\|^2/2}, \text{ where a point on the skeleton is denoted by } \mathbf{s}_i.$$

If  $S = \{\mathbf{s}_i\}$  is a set of infinitesimally spaced points,  $f$  can be expressed as an integral:

$$(6) \quad f(\mathbf{p}) = c - \int_S e^{-\|\mathbf{p} - \mathbf{u}\|^2/2} d\mathbf{u}, \text{ where } \mathbf{u} \text{ ranges over all points on the skeleton.}$$

Convolution is a process whereby a *signal* is modified by a *filter*. Here, the signal is a skeleton and the filter is a three-dimensional Gaussian *kernel*. Unlike algebraic surfaces, a blend is achieved by integration. The evaluation of the convolution integral is discussed

in [Bloomenthal and Shoemake 1991] and examined further in [Bloomenthal 1995].

In general, the frequency components of the signal are scaled by those of the filter. This can produce various results, but low-pass filtering, *i.e.*, the removal of high frequency components in the signal, is the most relevant to blending. When a signal is low-pass filtered, it loses detail and is said to be *smoothed*. For example, a two-dimensional image becomes blurred and objectionable creases, such as those in figure 1, are reduced or eliminated. The affect of a filter can be shown by the *Fourier transform*, which converts a signal (such as the kernel itself) into its frequency components. Interestingly, the Gaussian, shown below, is its own Fourier transform; thus, the upper frequencies of the original shape are attenuated to a gently increasing degree. We call the zero set of the smoothed function a *convolution surface*.

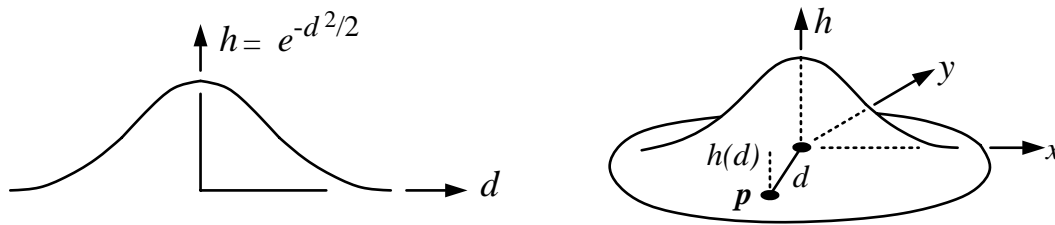


**Figure 5. Gaussian Kernels**

*left: one-dimensional, right: two-dimensional*

Convolution is well-known as an elegant solution to a wide range of application problems; here its elegance lies in its ability to smooth a shape without introducing bulges. This is due to its property of *superposition*. Because convolution is a linear operator, the sum of the convolutions of any division of a skeleton is identically equal to the single convolution of the entire skeleton. That is, using  $\otimes$  to represent convolution,  $h \otimes (s_1 + s_2) = (h \otimes s_1) + (h \otimes s_2)$ . This guarantees, for example, that two abutting, collinear segments produce the same convolution as does the single segment that is their union. Because of this property, we may convolve each skeletal element individually and sum the results. The division of a skeleton into small elements will not introduce any seam or bulge in the surface near the joins of the elements. This contrasts with algebraic blends, which can produce bulges near the joins of the skeletal primitives.

For example, the contours below illustrate the sum of two convolutions; the result is smooth regardless of the angle between segments. Along convex portions of the skeleton the surface mimics the union operator; along concave portions, the surface yields a blend. The intermediate contours smoothly interpolate the extrema. For isolated convex skeletons, such as triangles or segments, convolution produces surfaces of similar shape to distance surfaces. For complex skeletons, however, convolution yields crease-free surfaces with adjacent primitives blending without seam or bulge.

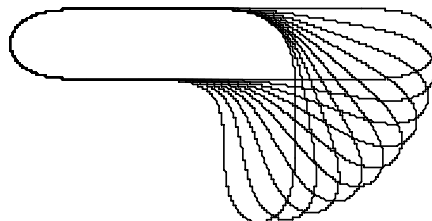


*Figure 6. Two Segments Convolved with the Gaussian Kernel*

## Other Kernels

Although the Gaussian is a satisfactory kernel, we also consider the B-spline and Wyvill kernels, both prominent in the literature [Bartels *et al.*], [Wyvill *et al.*]. The Gaussian is separable, but its integral must be numerically approximated. The B-spline and Wyvill kernels can be analytically integrated, but are not separable. Experiments with negatively-lobed filters (such as  $\sin(\pi x)/\pi x$ ) suggest monotonicity of the kernel is necessary for a satisfactory convolution surface; otherwise, the filter may introduce spurious contours, [Bloomenthal 1995].

The B-spline is given by a set of 4<sup>th</sup> order basis functions:  $(x+2)^3/6$  for  $x \in [-2, -1]$ ,  $(-3x^3-6x^2+4)/6$  for  $x \in [-1, 0]$ ,  $(3x^3-6x^2+4)/6$  for  $x \in [0, 1]$ , and  $(2-x)^3/6$  for  $x \in [1, 2]$ . The Wyvill is given by  $(9-4x^6+17x^4-22x^2)/9$ . The Gaussian has infinite support (although, in practice, there is negligible energy above 3), the B-Spline has a support of 2, and the Wyvill has a support of 1. All three kernels, when scaled so that  $h(0) = 1$  and  $h(1) = 1/2$ , are similarly shaped, as shown below.

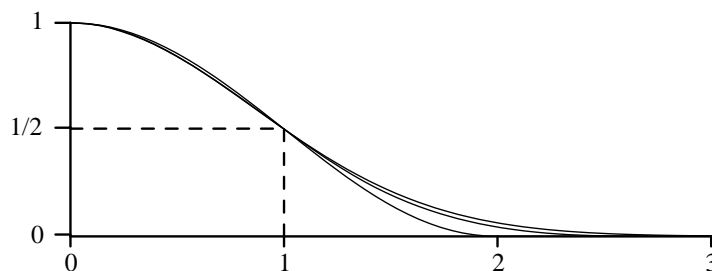


*Figure 7. Comparison of Filter Kernels*  
upper: Gaussian, middle: B-spline, lower: Wyvill

## Normalizations

If the exponent in equations (5) and (6) is scaled by  $\pi$ , the kernel will have unit integral. That is, the area under the curve (figure 5, left) and the volume under the surface (figure 5 right) will both be one. This implies that a signal modified by such a kernel will maintain its original energy. For example, if we convolve a box function (whose width exceeds the full filter support) with a unit integral kernel, the peak amplitude will equal the amplitude of the original box function. Or, if we convolve a two-dimensional image, the overall

energy in the image will be preserved. A kernel with integral less than one, however, would attenuate a signal; a kernel with integral greater than one would amplify the signal.



**Figure 8. Convolution of a Box Function**

Because the Gaussian is symmetric, the convolution equals  $\frac{1}{2}$  where the box function undergoes transitions. Thus, for an iso-surface contour level of  $\frac{1}{2}$ , the convolution surface will pass through the endpoints of skeletal segments and through the edges of skeletal polygons. Accordingly, we express the convolution surface as:

$$(7) \quad f(\mathbf{p}) = \frac{1}{2} - (h \otimes s)(\mathbf{p}).$$

### Ramification

Consider a distance surface given by a branching skeleton that is organized hierarchically into parent and child segments. The implicit surface function can be given as the parent segment function or the summation of the child segment functions, whichever is greater:

$$(8) \quad f(\mathbf{p}) = \max(f_{segment}(\mathbf{p}, parent), \sum_i^n f_{segment}(\mathbf{p}, child_i)),$$

where  $f_{segment}$  is some function of distance from  $\mathbf{p}$  to a segment and  $n$  is the number of child segments. To maintain continuity of radii, the radius of *parent* is scaled such that in the plane perpendicular to *parent*, at its endpoint,  $f_{segment}(parent) = \sum_i f_{segment}(child_i)$ . As a consequence of the summation in equation (8), the parent branch will be thicker than the individual child branches. This is another instance of bulging in implicit modeling. It is reasonable to ask whether convolution can solve the problem of ramiform bulge.

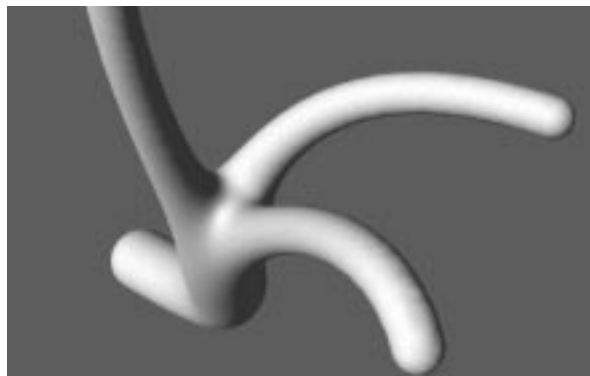


**Figure 9. A Trifurcated Ramiform**

We first examine a simple ‘tee’ skeleton, below, which consists of two segments. Each cylinder has radius  $r$ . Application of a Gaussian filter yields the following contours; the

dashed lines in the shaded images demarcate the isolated cylindrical primitives. Slight bulges at the segment junction are apparent in both planes.

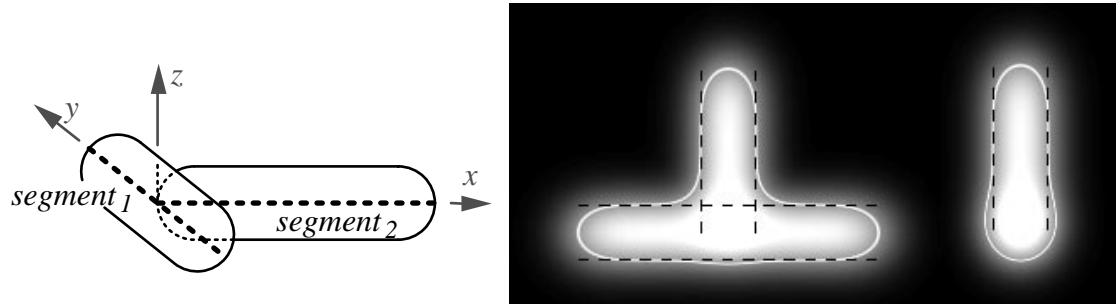


**Figure 10.** A 'Tee'

*left: skeletal geometry, middle: contour in  $xy$ -plane, right: contour in  $xz$ -plane*

To understand this phenomenon better, consider the behavior of  $f(\mathbf{p})$  for points  $\mathbf{p} = (x, 0, r)$ , shown below, left. As  $x$  increases and  $\mathbf{p}$  moves along the  $z = r$  line, the convolution of the two segments, measured at  $\mathbf{p}$ , changes. This is graphed in the figure below, right, and predicts the bulge at the junction of the two segments. Details of the computation are provided in [Bloomenthal 1995].

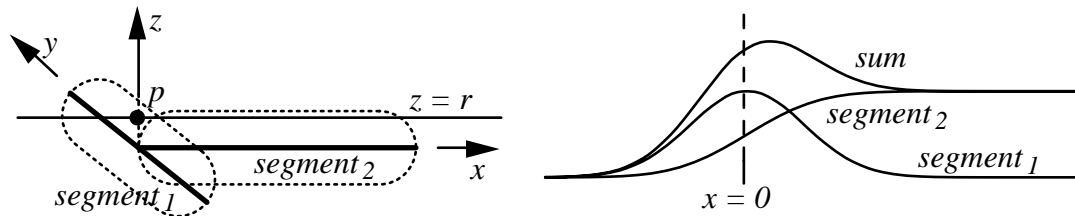


**Figure 11.** 'Tee' Junction with  $segment_1$  and  $segment_2$  Touching

## Bulge Reduction

It is possible to reduce the bulge by slightly separating the segments. If the left endpoint of  $segment_2$  is moved to the right by  $r$ , as shown below, the summation, although still not constant, shows less variation.

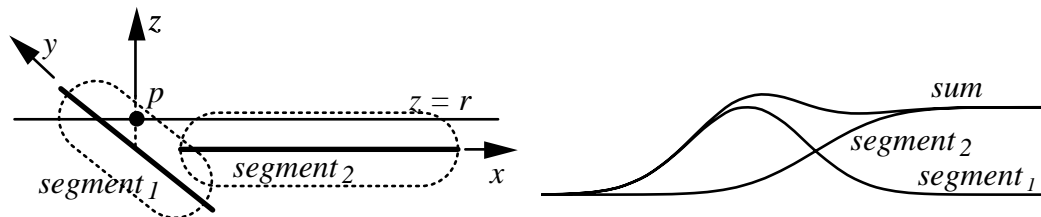


**Figure 12.** 'Tee' Junction with Shortened  $segment_2$

Shortening  $segment_2$  does, however, improve the appearance of the contours shown below. The bulge and dip predicted by the mathematical model, although subtle, are visible in the shaded surface.

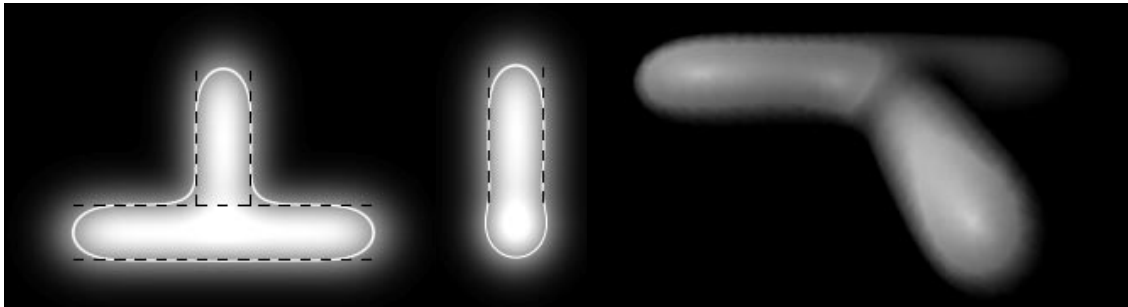


*Figure 13. Contours and Surface for the 'Tee' with Shortened Segment<sub>2</sub>*

### The Combination Surface

It would appear that we must blend when  $p$  is within the plane of the junction and avoid a bulge by not blending when  $p$  is out of the plane of the 'tee.' This 'combination surface' is reminiscent of equation (3) and is readily implemented for a skeleton by associating an approximating plane with each skeletal joint. The contribution of the 'union surface' can be derived from the angle between the plane normal and the vector from the joint to the  $p$ . In the figure below we compare the three types of surfaces.

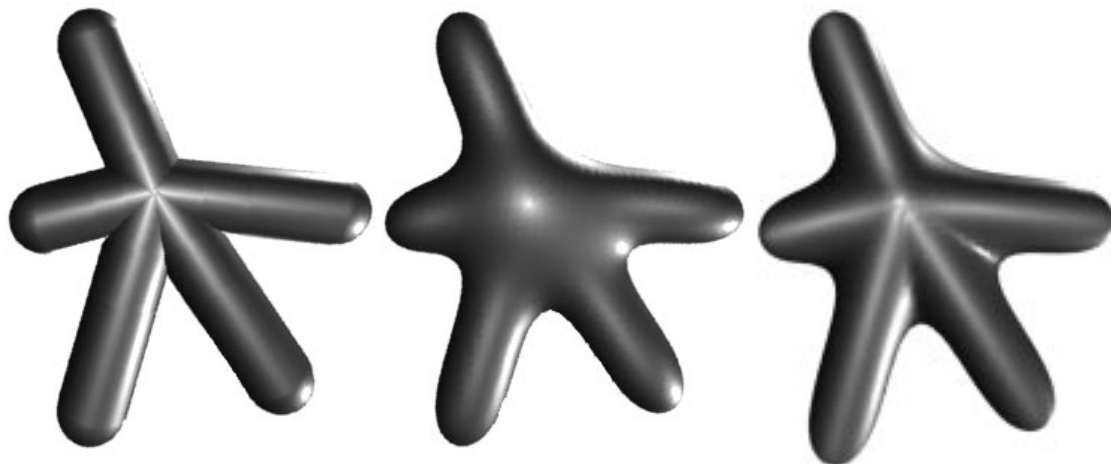


*Figure 14. Union Surface (left), Convolution Surface (middle), and Combination (right)*

The combination surface can be modified in several ways; we may, for example, experiment with the function that interpolates the union and convolution surfaces. Or, rather than fit a plane to the vertices of a joint, a free-form surface could be fit. As described in [Bloomenthal 1995], the webbing that blends together pairs of limbs in the combination surface will, necessarily, contain a small crease. This does not appear

objectionable in the above image, but prompts further investigation.

## Two Dimensional Skeletal Elements and Bulge Elimination

To accommodate objects with non-circular cross-sections, one-dimensional skeletal curves were extended to two-dimensional skeletal polygons [Bloomenthal and Shoemake 1991]. As with one-dimensional skeletal elements, the convolution surface for two-dimensional skeletal elements is evaluated as the sum of independent primitives. For example, the two polygons, below, left, yield the surface shown below, right.

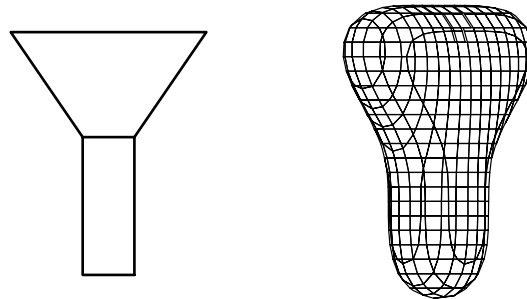


*Figure 15. Polygonal Skeleton (front view) and Convolution Surface (oblique view)*

A more sophisticated application of both one and two-dimensional skeletal elements, below, left, yields the surface shown below, right.

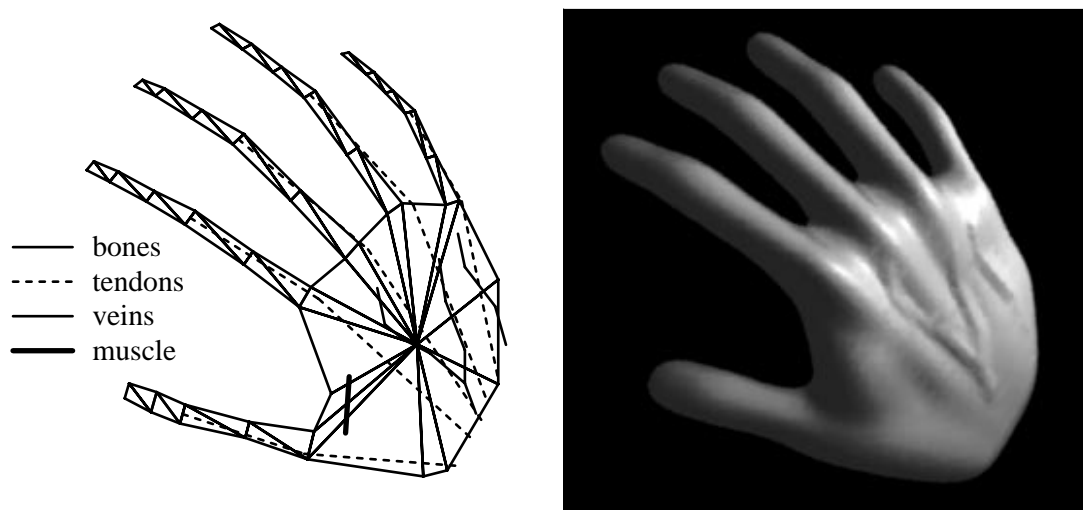


*Figure 16. Skeleton and Hand*

In the previous section we expressed dissatisfaction concerning the geometric quality of the combination surface developed to prevent bulges resulting from ramified skeletons. As seen in figure 11, a bulge is a consequence of increased skeletal density at the junction of the ramiform. In particular, an endpoint of  $segment_2$  touches  $segment_1$ , and the skeletal

density increases at this point. For polygons, a comparable arrangement might be two overlapping polygons, as shown below, left. We speculate that a contiguous (*i.e.*, abutting and non-overlapping) skeletal arrangement, such as below, right, alleviates the bulge.

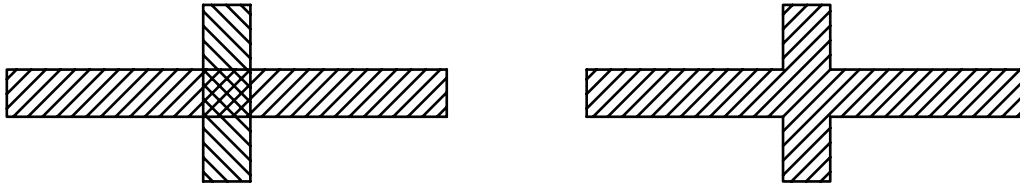


**Figure 17. Overlapped (left) and Contiguous (right) Skeletons**

To demonstrate this, and to explain the conditions under which it is true, we must examine the cross-section of a convolution surface derived from a polygon. As we observed in developing equation (7), the convolution surface of a polygon passes through the polygon edges. As shown below, different filter kernels require different polygon widths to produce equally thick surfaces.

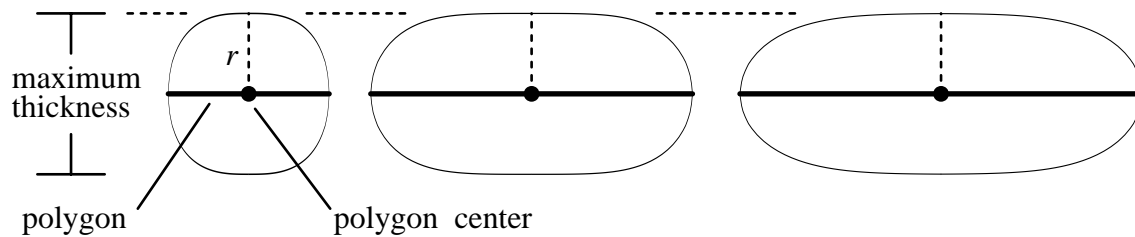


**Figure 18. Surface Cross-Sections for Different Kernels**

*left: Wyvill (width =  $2r$ ), middle: B-Spline ( $4r$ ), right: Gaussian ( $5r$ )*

For each of the filters shown above, the polygon width equals the effective support of the filter. This means the surface just reaches its maximal thickness at a point above the center of the polygon. Widening the polygon will not change the function value for points above the polygon center, but it will create a ‘plateau’ along the top and bottom of the surface, as shown below, left. If the polygon becomes narrower than the filter support, however, there is no point above the polygon for which the kernel, integrated over the polygon, can yield unity. This reduces the thickness of the surface, as shown below, right.

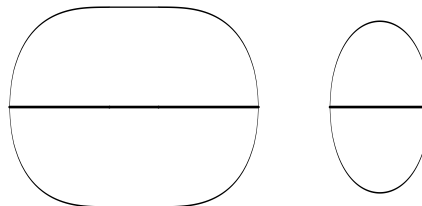


**Figure 19. Varying Polygon Width (Wyvill Kernel)**

*left: a wider polygon widens surface, right: a narrower polygon reduces object thickness*

Now, consider the contiguous skeletons shown below. For polygons whose width equals the support of the filter kernel, the entire filter (represented as a circle) projects onto the polygon, and the very centers of the polygons will yield a surface of maximal thickness. For the wider polygon, the region of maximal thickness will widen, creating a plateau. But for the narrower polygon, only at the junction center is there sufficient room for an entire kernel; elsewhere the kernel is clipped. A bulge will occur at the center of the junction of the narrow polygons, but not with the wider polygons.

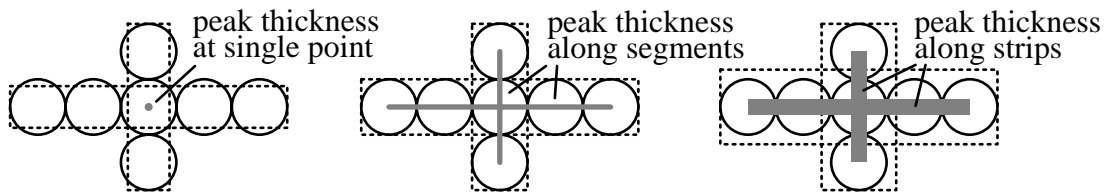


**Figure 20. Affect of Varying Polygon Width on Integration Filter**

*left: polygon width  $< 2r$ , middle: polygon width  $= 2r$ , right: polygon width  $> 2r$*

Thus, for an appropriate choice of polygon width, a contiguous polygonal skeleton yields ramiforms without bulge. The cross-sections of surfaces are not perfectly circular, however, unlike those for segments. The above skeleton is articulated, below.

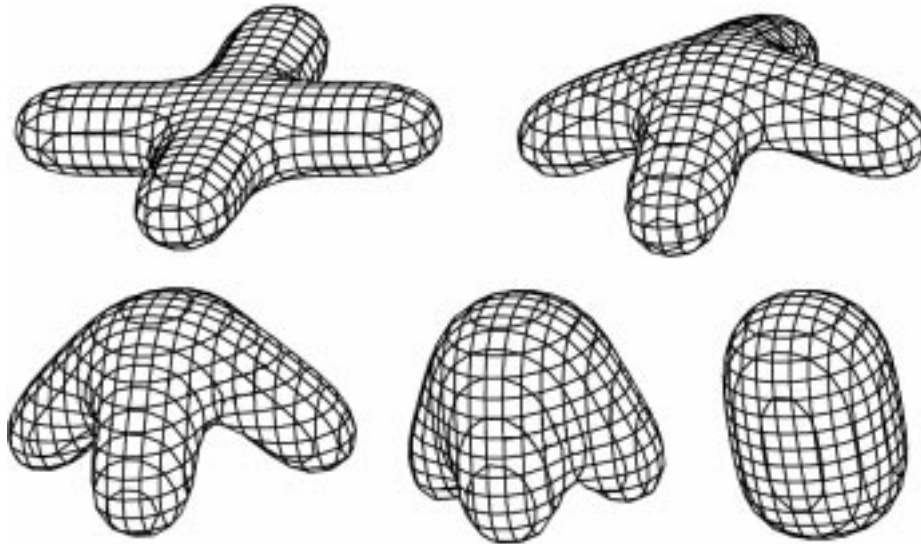


**Figure 21. A Smoothly Folding, Bulge-Free Form**

In the previous section we discussed the ‘plateau’ that develops over wide polygons. Because of the superposition property of convolution, this plateau may develop from an arbitrary configuration of coplanar, abutting polygons, and will be seamless. This seamlessness provides flexibility in the definition of polygonal skeletons, which we attempt to demonstrate in the following illustration.

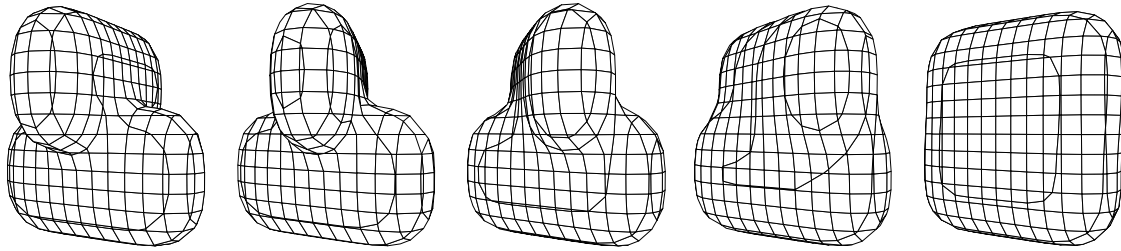


*Figure 22. Seamlessness*

## Conclusions

Because convolution is an integration, it produces a material blend of primitive volumes; the resulting object appears pliable. The object is not amorphous, however, because blending occurs only where skeletal elements are in proximity; the remainder of the surface closely follows the skeletal structure.

We dislike the popular term ‘blobby’ because it suggests something amorphous and without structure. The skeleton, however, is meant to provide structure, and, therefore, we prefer the term ‘blend.’



We speculate that one-dimensional segments and two-dimensional polygons provide great flexibility for the design of convolution surfaces, although the use of point and volumetric skeletons may also be appropriate for certain forms. As described in [Bloomenthal 1995], the convolution of a single point source may be performed analytically, the convolution of a segment requires analytical computation as well as a table for the Gaussian integral, and the convolution of a polygon requires a raster representation for the polygon. A practical implementation for the convolution of a volume would require a discrete, voxel representation.

Just as the use of polygons eliminates the bulge introduced by a corresponding skeletal structure based on segments, the use of volumes eliminates the bulge introduced by a corresponding skeletal structure based on polygons. In other words, to avoid bulges in implicit blends, a skeleton should be locally manifold. For a one-dimensional skeleton, this means there should be no points incident to a segment; for a two-dimensional skeleton, there should be no edge incident to a polygon. A comparison is given below.



*Figure 23. One, Two, and Three-Dimensional Skeletons  
left: those that produce bulges, right: those that do not*

A design environment utilizing convolution surfaces enables the creation of complex, well-behaved shapes through the specification of skeletal elements. In using convolution, however, the designer loses explicit control over fillets and chamfers. This is more than compensated by the generality of convolution blending. Resulting surfaces are smooth and are bulge-free provided the skeletal elements are contiguous and, collectively, at least as wide as the full filter support.

## Acknowledgments

My thanks to Paul Heckbert, Przemek Prusinkiewicz, and Brian Wyvill. Their help has been greatly appreciated.

## References

- R. Bartels, J. Beatty, and B. Barsky, *An Introduction to Splines for use in Computer Graphics and Geometric Modeling*, Morgan Kaufmann Publishers, Los Altos CA, 1987.
- James Blinn, *A Generalization of Algebraic Surface Drawing*, ACM Transactions on Graphics, July 1982).
- Jules Bloomenthal, *Techniques for Implicit Modeling*, Xerox PARC Technical Report P89-00106, 1989.
- Jules Bloomenthal, *Skeletal Design of Natural Forms*, Ph.D. dissertation, Department of Computer Science, University of Calgary, 1995.
- Jules Bloomenthal and Ken Shoemake, *Convolution Surfaces*, Proceedings of SIGGRAPH'91, Las Vegas, NV, in Computer Graphics 25, 4, July 1991.
- Christoph Hoffmann and John Hopcroft, *The Potential Method for Blending Surfaces and Corners*, Technical Report TR 85-674 Computer Science Dept., Cornell University, 1985.
- A. E. Middleditch and K. H. Sears, *Blend Surfaces for Set Theoretic Volume Modeling Systems*, Proceedings of SIGGRAPH'85, San Francisco, CA, in Computer Graphics 19, 3, July 1985.
- Alyn Rockwood, *The Displacement Method for Implicit Blending Surfaces in Solid Models*. ACM Transactions on Graphics 8, 4, October 1989.
- A. Rockwood and J. C. Owen, *Blending Surfaces in Solid Modeling*, Proceedings of SIAM Conference on Geometric Modelling and Robotics, G. Farin, editor, Albany, NY, 1985.
- Philip Schneider, *Solving the Nearest-Point-On-Curve Problem*, in Graphics Gems, Andrew Glassner, editor, Academic Press, New York, 1990.
- J. R. Woodwark, *Blends in Geometric Modelling*, Proceedings of the 2nd IMA Conference on the Mathematics of Surfaces, Cardiff, September 1986.
- G. Wyvill, C. McPheeters, and B. Wyvill, *Data Structure for Soft Objects*. Visual Computer 2, 4, August 1986.